JGR Atmospheres

RESEARCH ARTICLE
10.1029/2023JD039610

Exploring Deposition Observations of Oxidized Sulfur and Nitrogen as a Constraint on Emissions in the United States

Ishir Dutta[1] and **Colette L. Heald**[1,2]

[1]Department of Earth, Atmospheric and Planetary Sciences, Massachusetts Institute of Technology, Cambridge, MA, USA, [2]Department of Civil and Environmental Engineering, Massachusetts Institute of Technology, Cambridge, MA, USA

Key Points:

- The GEOS-Chem model captures the substantial decrease in deposition of sulfur oxides and inorganic nitrate over the United States from 1990 to 2021
- Derived dry deposition observations constrain local anthropogenic emission trends, while wet deposition measurements reflect total sources
- The GEOS-Chem model is unable to simultaneously replicate ambient and deposited nitrate, providing evidence for under-explored sinks of NO_y

Supporting Information:

Supporting Information may be found in the online version of this article.

Correspondence to:

I. Dutta and C. L. Heald,
idutta@mit.edu;
heald@mit.edu

Citation:

Dutta, I., & Heald, C. L. (2023). Exploring deposition observations of oxidized sulfur and nitrogen as a constraint on emissions in the United States. *Journal of Geophysical Research: Atmospheres*, *128*, e2023JD039610. https://doi.org/10.1029/2023JD039610

Received 7 JUL 2023
Accepted 27 OCT 2023

Author Contributions:

Conceptualization: Colette L. Heald
Data curation: Ishir Dutta
Formal analysis: Ishir Dutta
Funding acquisition: Colette L. Heald
Investigation: Ishir Dutta, Colette L. Heald
Methodology: Ishir Dutta, Colette L. Heald
Project Administration: Colette L. Heald
Resources: Colette L. Heald
Supervision: Colette L. Heald
Visualization: Ishir Dutta

Abstract Emissions of anthropogenic sulfur and nitrogen oxides form secondary pollutants that impact human health, ecosystems, and climate. Accurate estimates of emissions trends are needed to verify the effectiveness of the regulation of these species. We explore the utility of deposition measurements of SO_x (=SO_2 + SO_4^{2-}) and TNO_3 (=HNO_3 + NO_3^-) as constraints on emissions trends of SO_x and NO_x in the conterminous United States (CONUS) from 1990 to 2021. The GEOS-Chem model captures observed annual SO_x and TNO_3 wet deposition at NADP-NTN sites in 2011 with a −15% and +15% normalized mean bias (NMB), respectively. The model overestimates the dry deposition of SO_x and TNO_3 estimated at CASTNET sites in 2011 (NMB >100%), however, this bias is substantially reduced when using an alternate derived dry deposition data set at the same sites, highlighting the uncertainty in dry deposition velocities. Despite this, we find that the model (driven by scaled NEI emissions) captures the relative trend in dry deposition of SO_x (−93% observed and −94% simulated) and TNO_3 (−66% observed and −68% simulated) from 1990 to 2021 and that these decreases closely reflect the trends in anthropogenic SO_2 emissions (−93%) and anthropogenic NO_x emissions (−71%), respectively. SO_x and TNO_3 wet deposition observations are dominated by soluble secondary products and are more influenced by natural and transboundary sources, and therefore have decreased more modestly over the same period (−78% and −52%). Natural sources of NO_x are relatively constant during this time and therefore moderate the reduction in total NO_x emissions (−55%).

Plain Language Summary Sulfur and nitrogen oxides (SO_x and NO_x) are emitted into the atmosphere by a variety of natural and anthropogenic source and have significant impacts on ecosystems, human health, and climate. These wide-ranging effects have made these compounds the subject of sweeping regulatory action in the United States, thereby requiring an accounting of the changes in their emissions over time. However, such an accounting is challenged by the wide range of emission sources and the complexity of SO_x and NO_x chemistry in the atmosphere. These pollutants are ultimately removed either by precipitation (wet deposition) or by uptake by land and vegetation (dry deposition). In this work, we explore whether a continuous, consistent, spatially heterogeneous data set (observed wet deposition and derived dry deposition) in the United States over several decades is able to constrain trends in SO_x and NO_x emissions. We find that secondary pollutant dry deposition estimates follow the trend in local anthropogenic emissions of SO_x and NO_x, and that wet deposition measurements reflect the trend in total regional emissions (anthropogenic, natural, and transboundary). We conclude that deposition measurements can be a useful constraint on the long-term trends in emissions of environmental pollutants, even when complex atmospheric chemistry is involved.

1. Introduction

Sulfur and nitrogen are emitted into the atmosphere by a wide range of natural and anthropogenic sources, where they are subject to gas and particle phase chemistry and transport, forming secondary pollutants that have deleterious effects on air quality, ecosystems, and climate. These effects include acid rain (Likens & Bormann, 1974), eutrophication (Bouwman et al., 2002; Schindler, 1974), ozone formation (Haagen-Smit, 1952), and secondary aerosol formation (Seinfeld & Pandis, 1998), with secondary inorganic aerosol contributing to approximately half of fine particulate matter ($PM_{2.5}$) in the United States in the early 2000s (Bell et al., 2007). Air pollution is one of the primary contributors to the global burden of disease (Dockery et al., 1993; C. J. L. Murray et al., 2020) and is regulated in the United States by the Clean Air Act and its subsequent amendments, leading to an estimated 92% decrease in emissions of sulfur dioxide (SO_2) and a 68% decrease in emissions of nitrogen oxides (NO_x = NO + NO_2) from 1990 to 2020 (US EPA, 2021).

Writing – original draft: Ishir Dutta, Colette L. Heald
Writing – review & editing: Ishir Dutta, Colette L. Heald

A robust understanding of the trends in emissions is required to understand the impacts of existing legislation targeting nitrogen and sulfur emissions, as well as to inform effective future regulation that seeks to further improve air quality. At present, our best estimates come from emissions inventories. These inventories are built from the bottom-up, requiring the survey and accounting of a wide array of emitters, from point sources (e.g., power plants) to distributed sources (e.g., agriculture) to mobile sources (e.g., vehicles). The expansive nature of this undertaking makes producing an emissions inventory extremely resource-intensive. The United States Environmental Protection Agency (US EPA) National Emissions Inventory (NEI), for instance, is updated only every 3 years, and the underlying methods and models used to integrate local and state data into national emissions estimates are subject to change with each iteration (US EPA, 1998, 2001b, 2015). The evolving nature of bottom-up emissions estimates can lead to abrupt transitions in emission inventories over time, which challenges the assessment of continuous trends in emissions, as it requires a backward-compatible analysis of emissions. Recent work by the EPA's Air QUAlity TimE Series Project has begun to address some of these concerns by producing a consistent, continuous set of emissions data for 2002–2017 (Foley et al., 2023).

Top-down assessments, based on observed concentrations or fluxes, provide a complementary approach to constraining emissions. These range from the continental-scale (e.g., satellites) to the hyper-local (e.g., eddy flux measurements). However, as with bottom-up estimates, these top-down constraints are not without their limitations. For example, while satellite measurements allow for large-scale, near-real-time information, they provide information about the concentrations of a limited number of species of interest, and require inverse modeling frameworks to estimate source-apportioned emissions from observed concentrations. At a smaller scale, eddy flux measurements from both surface stations and aircraft are able to provide a great deal of granularity, though separation of emission and deposition processes can be challenging. Both satellite and in situ eddy covariance measurements are spatially and/or temporally limited, and therefore cannot provide multi-decadal trends at the scale of a state or country.

Observed deposition may provide a complementary constraint on emissions as atmospheric trace species have a finite atmospheric residence time, and physical deposition can be the dominant loss pathway for some atmospheric constituents. In the 1970s, with rising concerns about air quality and acid rain, the United States established the first 22 sites of what would eventually become the National Atmospheric Deposition Program's National Trends Network (NADP-NTN) to measure precipitation chemistry by collecting weekly, wet-only samples. The network has grown to >250 active (largely rural) sites. A complementary network, the Clean Air Status and Trends Network (CASTNET), was established under the 1990 Clean Air Act Amendments to study ambient ozone and acid dry deposition. It currently has ∼100 active sites, which operate on the same sampling schedule as NADP-NTN. Together, these networks have monitored long-term, continuous, spatially heterogeneous deposition trends in the Unites States (Nopmongcol et al., 2019; Sickles & Shadwick, 2015).

Although deposition is the final step in a complex cascade of transport and chemistry, previous work has used deposition data and inverse models to exploit the relationship between deposition and emissions (Gilliland et al., 2003, 2006), and back-trajectories to establish a near-linear relationship between the response of deposition of sulfate and nitrate downwind to the emission of SO_x and NO_x upwind (Butler et al., 2001, 2003). Nopmongcol et al. (2019) modeled a 1.0%–1.7% a^{-1} decline in sulfur deposition, and a 0.6%–1.4% a^{-1} decline in NO_y deposition between 1970 and 2020, comparable to a 1.4%–1.8% a^{-1} reduction in SO_2 emissions and a 0.5%–1.6% a^{-1} reduction in NO_x emissions in the same period. However, while there have been efforts to use deposition data in conjunction with a chemical transport model to improve emissions estimates (Kim et al., 2015; Paulot et al., 2014) and to evaluate the performance of models (Park et al., 2004; L. Zhang et al., 2012), there has not been a comprehensive evaluation and comparison of the trends in emissions estimates and observed deposition against deposition as modeled by a state-of-the-science chemical transport model.

Here, we explore whether and under what conditions deposition measurements of SO_x ($=SO_2 + SO_4^{2-}$) and TNO_3 ($=HNO_3 + NO_3^-$) can be used as a constraint on anthropogenic emissions trends of SO_x and NO_x in the conterminous United States (CONUS). Both SO_x and TNO_3 are primarily physically removed, with lifetimes to deposition on the order of a week. Given that the mean transport time of an air mass traveling across the United States is also on the order of a week, we expect that a significant fraction of CONUS-origin SO_x and TNO_3 will be deposited within CONUS, and that the trends in deposition may be a good proxy for trends in emissions (see Section 3.2 for a more complete discussion). We focus here on SO_x and TNO_3 wet deposition which responds strongly to changes in emissions; Benish et al. (2022) and Tan et al. (2020) show that NH_x deposition response to emission

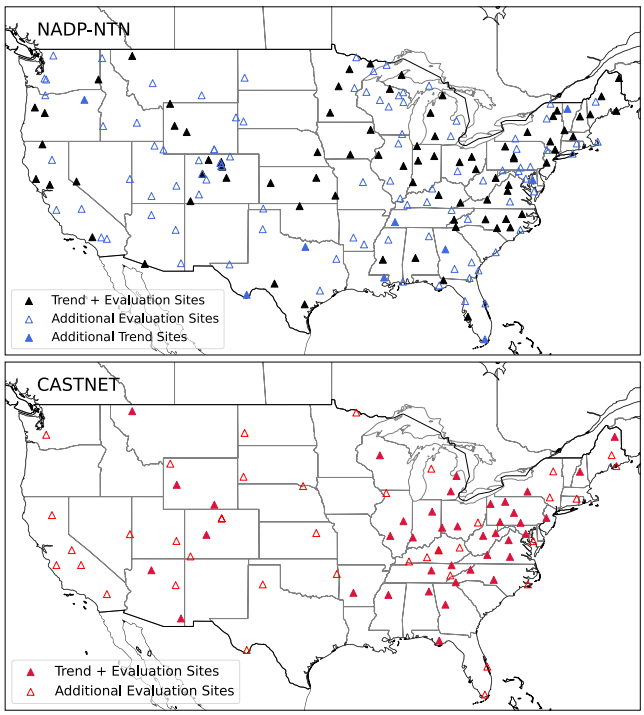

Figure 1. Locations of National Atmospheric Deposition Program's National Trends Network (NADP-NTN) (blue) and Clean Air Status and Trends Network (CASTNET) (red) sites in conterminous United States that meet completeness and continuity criteria (described in Section 2.1). Each panel shows all sites used for both the 2011 evaluation and the trend analysis (solid dark symbols), as well as additional sites used solely in the evaluation (empty symbols), or in the trend analysis (solid light symbols).

abatement is more complex, reflecting the critical role of thermodynamic partitioning in controlling NH_x. We first use deposition data to evaluate the GEOS-Chem chemical transport model's representation of deposition magnitude and speciation, and subsequently use the observations and GEOS-Chem to study the trends in emission and deposition of these species over time.

2. Materials and Methods

2.1. NADP-NTN Wet Deposition Network

The NADP-NTN measures wet deposition in the United States. Collection buckets lined with sampling bags provided by the Central Analytical Laboratory (CAL) at the University of Wisconsin-Madison are installed at each NTN site on a weekly basis, where they are deployed with a rain gauge (reporting precipitation to the nearest 0.01 in) and are set to automatically open only during precipitation and close immediately after. Samples are collected weekly on Tuesday mornings, weighed, and sent back to the CAL for analysis. Precipitation samples are tested for acidity (pH), conductivity, and concentrations of anion and cations (SO_4^{2-}, NO_3^-, NH_4^+, Cl^-, K^+, Na^+, Ca^{2+}). The bulk, integrated collection of precipitation does not allow the measurements to distinguish between gas phase and particle phase deposition, therefore, all SO_x is measured as SO_4^{2-} and all TNO_3 is measured as NO_3^-. For measurements of SO_4^{2-} and NO_3^-, the network method detection limit has historically ranged from 0.04 to 0.030 mg/L and is currently 0.018 mg/L (NADP, 2021a), which is approximately 1%–7% of the mean weekly deposition at a given site in CONUS. The reported mg/L and precipitation (cm) values are multiplied, accounting for the fraction of N and S in each deposited ion, to convert to a standardized deposition flux of kg-[N or S]/ha.

Sites have been added to the NADP-NTN since its inception in the 1970s; however, samples are not consistently collected year-round at all sites. We use the three completeness criteria recommended by the NADP (NADP, 2021b) to assess whether or not to include any given site in our analysis: (a) there must be valid samples (valid samples also include zero value samples collected during periods of trace or no precipitation) for >75% of the summary period (e.g., seasonal or annual), (b) precipitation (including zero) must be recorded by the sample volume or the rain gauge for >90% of the summary period, and (c) valid samples need to account for >75% of the precipitation recorded during the summary period. We use a subset of 175 sites that operated during 2011 and met all three criteria for the model evaluation (Section 3.3). For the trend analysis (Section 3.4), we used data from 88 sites that met the same completeness criteria and operated for at least 80% of the period (26 years or more between 1990 and 2021) (Benish et al., 2022; Y. Zhang et al., 2019) (Figure 1).

2.2. Clean Air Status and Trends Network

CASTNET reports dry deposition fluxes measured indirectly from ambient gas and particle phase concentration measurements. Ambient concentrations for sulfur dioxide (SO_2), sulfate (SO_4^{2-}), nitrate (NO_3^-), and nitric acid (HNO_3), as well as additional species not explored in this study, are measured by passing air at a steady flow rate through a sequence of three filters (a Teflon filter, a nylon filter, and a K_2CO_3-treated cellulose filter) mounted to sampling head 10 m above the ground. SO_4^{2-} and NO_3^- are measured from the Teflon filter; HNO_3 is measured as NO_3^- from the nylon filter; and SO_2 is measured as SO_4^{2-} from the nylon and cellulose filters. As in the case of the NADP-NTN, filters are replaced on Tuesdays and sent to the CAL for analysis. "Blank" filters are also sent every month to account for contamination during transport and the passive collection of species of interest. Ion chromatography with a Dionex ICS-1600 is used to measure SO_4^{2-} and NO_3^-. The analytical detection limits for CASTNET sites are 0.040 μg/mL for sulfate, 0.008 μg-N/mL for nitrate. Atmospheric concentrations from which deposition fluxes are calculated are considered valid if the filter pack flow represents hourly averages at least

75% of the sampling period, and samples with 75%–90% valid flow data are flagged to indicate uncertainty in the concentration calculations (CASTNET, 2020).

An estimate of deposition velocity is required to convert from the filter pack concentration measured at CASTNET sites to a dry deposition flux. Historically dry deposition velocities were estimated using a multi-layer model (MLM) (Finkelstein et al., 2000; Meyers et al., 1998). The deposition velocity is a function of chemical composition, meteorological conditions, and vegetation. However, since 2012 meteorological measurements are only taken at five EPA-sponsored sites, all National Park Service-sponsored sites and all Bureau of Land Management-sponsored sites, with the remaining sites using weekly hourly-average deposition velocities based on historical annual means to capture diurnal and seasonal cycles (Bowker et al., 2011). Since 2017, CASTNET has generated "total annual deposition" (Tdep) reports (Schwede & Lear, 2014) using output from the Community Multiscale Air Quality Modeling System (CMAQ), merged with meteorology observed at select sites to estimate weekly deposition velocities. However, these reports only include data for the period 2000–2020. Thus, to explore the 1990–2021 trend, we use the legacy MLM-derived weekly fluxes (available from 1987 to 2022) in this study. We find interannual variability, but no strong trend in the MLM deposition velocities over our study period, indicating that the observed trends in dry deposition fluxes over time are the result of trends in measured concentrations, which are driven by emissions (see Section 3.4). We note that previous work has shown that the CMAQ-based fluxes are substantially higher (by a factor of approximately 1.6 for HNO_3 and 2.6 for SO_2) than those reported for the same years using the MLM-based approach (Schwede & Lear, 2014). This highlights that the uncertainty in estimated dry deposition fluxes from observed concentrations is high and that our dry deposition flux "observations" are not well-constrained. We further discuss the implications of this uncertainty in Section 3.3. Weekly deposition flux values are reported as kg-[N or S]/ha.

2.3. Model Description

We use v13.3.4 of the GEOS-Chem global chemical transport model (www.geos-chem.org), driven by Modern-Era Retrospective analysis for Research and Applications, Version 2 (MERRA-2) assimilated meteorology. We perform simulations for 1990, 1996, 2001, 2006, 2011, 2016, and 2021 with a 6-month spin-up, at a horizontal resolution of 2° latitude by 2.5° longitude, 47 vertical hybrid-sigma levels, and a chemistry timestep of 20 min and transport timestep of 10 min (Philip et al., 2016). The global model output is used to generate boundary conditions for a nested grid simulation (Y. X. Wang et al., 2004) at a resolution of 0.5° latitude by 0.625° longitude over North America (20°N–55°N, 60°W–130°W), with a chemistry timestep of 10 min, and a transport timestep of 5 min. The model includes a simulation of HO_x-NO_x-VOC-O_3-halogen chemistry (Bates & Jacob, 2019; X. Wang et al., 2021) coupled to aerosol thermodynamics (Park et al., 2004; Pye et al., 2009). Partitioning of total ammonia and nitric acid between the gas and aerosol phases is calculated using the ISORROPIA II model (Fountoukis & Nenes, 2007).

Anthropogenic emissions (including ship emissions) follow the year-specific global Community Emissions Data System inventory (CEDSv2) (Hoesly et al., 2018; McDuffie et al., 2020), and are over-written by the monthly mean 2011 NEI (NEI 2011) (Travis et al., 2016) over the United States (annual scaling described below). We use the Global Fire Emissions Database (GFED4.1s) for biomass burning emissions between 1997 and 2019, with biomass burning emissions set to 1997 for the 1990 and 1996 simulations, and set to 2019 for the 2021 simulation. Dust (Fairlie et al., 2007; Ridley et al., 2012), biogenic VOCs (Guenther et al., 2012; Hu et al., 2015), sea salt, soil NO_x (Hudman et al., 2012) and lightning NO_x (L. T. Murray et al., 2012) are specified from offline year-specific archived emissions (Weng et al., 2020). Methane concentrations for the 2021 simulation used 2020 input files.

For year-varying NEI emissions within GEOS-Chem, an anchor year (here, 2011, shown in Figure 2) is scaled by applying national annual scale factors for NO_x, SO_2, NH_3, CO, VOC, OC, and BC (OC and BC use identical scale factors for carbonaceous aerosol from $PM_{2.5}$ emissions estimates), which are calculated from the EPA National Tier 1 Criteria Air Pollutants Trends report (US EPA, 2022). Additional scale factors are used within the default model to account for the day of week and the weekend effect (NEI 99) (US EPA, 2001a); and the diurnal cycle of NO_x, CO, OA, and VOCs (Janssens-Maenhout et al., 2011). To account for some of the spatial heterogeneity seen in emissions trends around the country, we replace the national annual scale factors with state-wise scale factors for NO_x, SO_x, NH_3, CO, VOCs, and $PM_{2.5}$, calculated from the same report by summing emissions from all sources, excluding wildfires and prescribed fires (Figure S1 in Supporting Information S1). We find

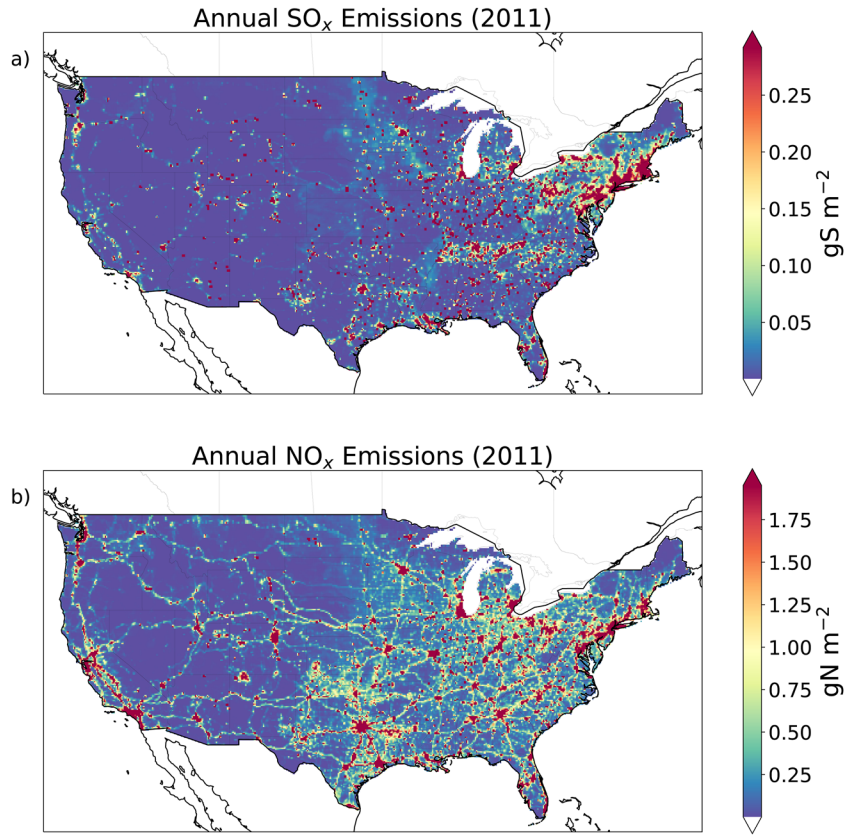

Figure 2. Annual anthropogenic emissions (NEI 2011) for (a) SO_x and (b) NO_x. The color bar saturates at 0.3 gS/m^2 for SO_x, and the figure has a maximum value of 317.7 gS/m^2. The color bar for NO_x saturates at 2.0 gN/m^2, and the figure has a maximum value of 108.9 gN/m^2.

that our method of scaling emissions state-wise results in national emissions totals that are within 2% (SO_x) and 4% (NO_x) of the standard national scaling approach. However, our more disaggregated scaling produces large regional differences in emissions. For example, national scaling causes SO_x emissions reductions between 1990 and 2021 to be underestimated by >48% in West Virginia, Tennessee, and New York; and overestimated by >127% in Texas, Louisiana, and Oklahoma. Similarly, national scaling results in reductions of NO_x emissions between 1990 and 2021 to be underestimated by >30% in California, New York, Pennsylvania, and Ohio; and overestimated by >88% in Oklahoma, Arkansas, Nebraska, and Colorado, and overestimated by >25% in Texas. Emissions totals for the CONUS for NO_x and SO_x in 1990, 2011, and 2021 are given in Table 1. When comparing our NEI baseline simulation with a simulation using NEI 2016 (Henderson & Freese, 2021) (nationally scaled to 2011), we find that NEI 2011 has ~20% higher SO_x emissions (largely in the northeastern U.S.), and 4% higher NO_x emissions (with no distinct regional differences), consistent with previous work (Freese et al., 2023). However, for the purposes of this work, the absolute differences in emissions are less important than the relative trends in emissions over time.

Table 1
SO_x and NO_x Emissions Over the Conterminous United States

		1990	2011	2021
NO_x (Tg N year^{-1})	Total	7.64	5.06	3.39
	Anthropogenic	6.64	3.63	1.96
	Aircraft	0.16	0.16	0.16
	Ships	0.02	0.03	0.03
	Biomass burning	0.031	0.055	0.035
	Lightning	0.41	0.51	0.54
	Soil	0.37	0.67	0.66
SO_x (Tg S year^{-1})	Total	10.92	3.01	0.89
	Anthropogenic	10.85	2.90	0.83
	Ships	0.04	0.07	0.03
	Aircraft	0.02	0.02	0.02
	Biomass burning	0.008	0.014	0.008

Wet deposition in GEOS-Chem includes two mechanisms—the scavenging of gases and aerosol by wet convective updrafts, and their removal by large-scale precipitation, as described by Liu et al. (2001) for water-soluble aerosols, and Amos et al. (2012) for gases. Removal by precipitation may occur in-cloud ("rainout") or below-cloud ("washout"). The sum of modeled wet loss by convective scavenging and loss by precipitation through the

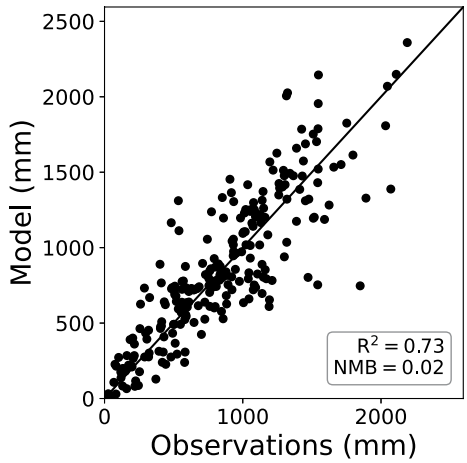

Figure 3. Model-measurement comparison of annual total precipitation in 2011 at National Atmospheric Deposition Program's National Trends Network measurement sites. The 1:1 line is in black; statistical comparison metrics are shown inset.

vertical column is compared to measured wet deposition at the surface. In addition to the standard model simulation, we also perform a set of simulations which include the updates to the wet deposition scheme following Luo et al. (2019, 2020). These updates include the use of spatially and temporally varying in-cloud condensed water (which is ∼5 times lower over CONUS in the summer and ∼2 times lower in the winter than the previously assumed constant value), and a higher empirical washout rate for nitric acid, which is two orders of magnitude above the previous value. We focus the majority of our analysis on the default scheme, with comparisons using the Luo et al. updates provided in our model evaluation section (Section 3.3).

Dry deposition is represented by a resistances-in-series model (Wesely, 1989), implemented by Y. Wang et al. (1998), with size-dependent aerosol dry deposition from Emerson et al. (2020) which is based on L. Zhang et al. (2001). Dry deposition depends on land cover type, local meteorology, and the reactivity, solubility and hygroscopic growth rate of the gases or particles being deposited.

Daily model output is sampled at all the NADP-NTN and CASTNET sites and aggregated up to match the measured weekly Tuesday-to-Tuesday integrated samples that meet the specified completeness criteria (Sections 2.1 and 2.2).

3. Results and Discussion

We use wet deposition measurements from NADP-NTN and derived dry deposition from CASTNET along with the GEOS-Chem model to explore the relationship between emissions and deposition over time in the United States. We evaluate precipitation, describe and evaluate the model simulations of SO_x and TNO_3 deposition, and then discuss trends in emissions and deposition.

3.1. Precipitation

To meaningfully interpret differences between observed and simulated deposition, we first evaluate the MERRA-2 precipitation which drives the GEOS-Chem CTM against the weekly samples collected at NADP-NTN sites. Figure 3 shows that over the course of our anchor year (2011), total annual precipitation is well represented across the NTN sites ($R^2 = 0.73$, normalized mean bias [NMB] = 2%). Weekly precipitation samples show higher variability, as expected, which the model is less skilled in representing ($R^2 = 0.37$); however, the MERRA-2 precipitation remains relatively unbiased (NMB < ±9%) across seasons. There is no significant trend in precipitation volume over the study period in either the observations or model, and model skill is similar across all simulated years.

3.2. Simulated SO_x and TNO_3 Deposition

We find that in our simulations, the leading simulated SO_2 oxidation pathways to form sulfate over the United States are, in order of importance, oxidation by in-cloud O_3, gas phase OH, and in-cloud H_2O_2. We note a slight increase (<10%) in the relative importance of the in-cloud O_3 pathway in the GEOS-Chem simulation over the last three decades, and both findings are consistent with previous work (Hattori et al., 2021). Geographically, SO_x deposition peaks in the eastern US (Figure 4a), downwind of SO_x emissions (Figure 2a). Figures 4c and 4e also show that simulated dry deposition of SO_x (which is dominated by primary SO_2) is localized close to source, whereas wet deposition (which is dominated by secondary sulfate) is more diffuse downwind of sources. The simulated sulfur lifetime to deposition is 2–5 days, varying seasonally (with shortest lifetimes in the summer, largely driven by the seasonality in SO_2 dry deposition).

Figure 2b highlights the greater spatial heterogeneity of anthropogenic NO_x emissions in CONUS, as point sources that co-emit SO_x are supplemented by on-road and non-road mobile sources. There are also more salient natural (e.g., soil, lightning, see Table 1) and transboundary sources of NO_x. The resulting simulated TNO_3 deposition is

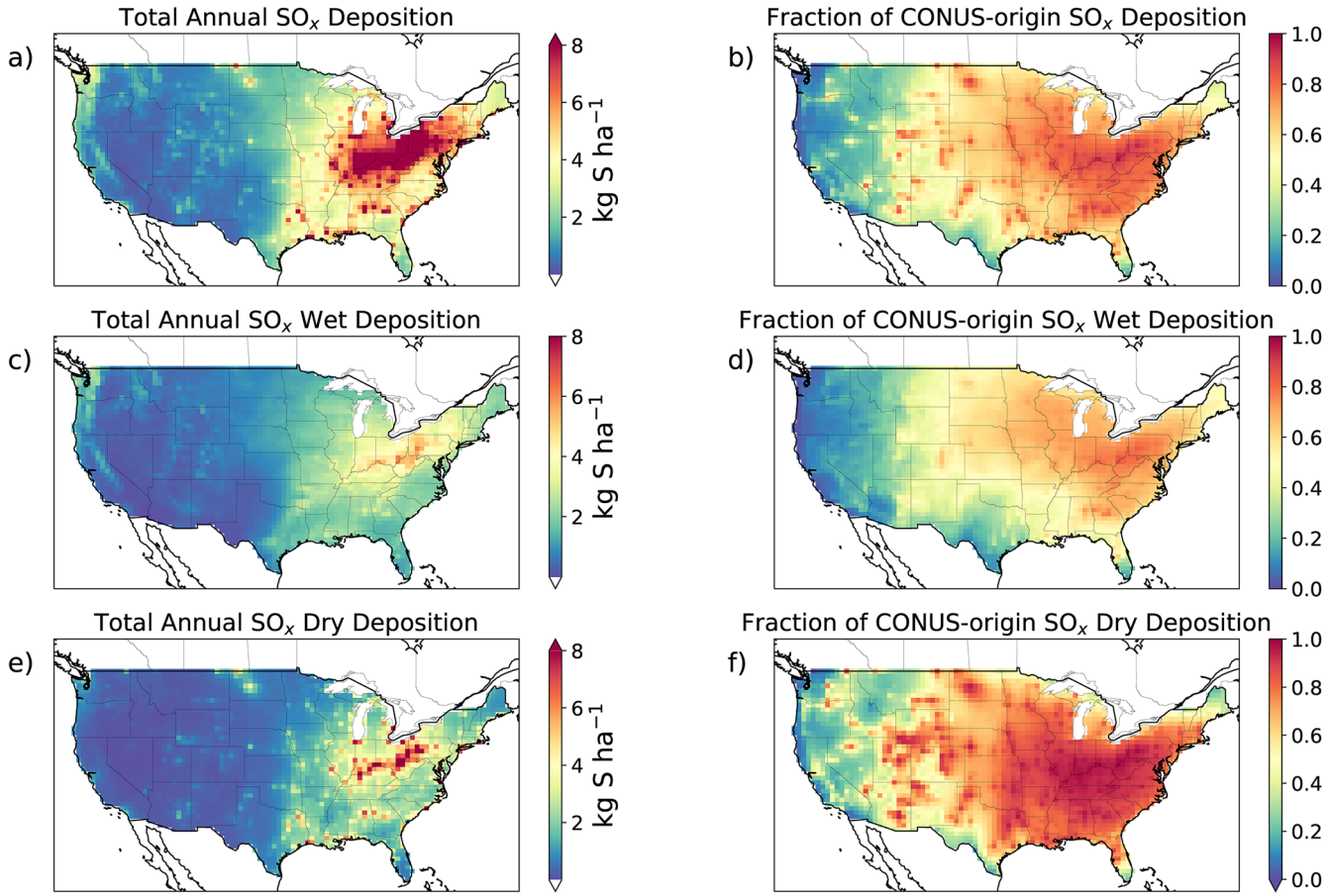

Figure 4. GEOS-Chem simulation of (a) total, (c) wet, and (e) dry annual mean SO_x deposition in 2011, and (b, d, f) fractions of simulated SO_x deposition originating from conterminous United States (CONUS) anthropogenic sources.

shown in Figure 5a. Figures 5c and 5e show a similar pattern to the SO_x system, where wet deposition of TNO_3 is more diffuse than dry deposition. The seasonality of TNO_3 deposition is similar but stronger than that of SO_x, with the lifetime to deposition for TNO_3 being driven by HNO_3, varying between 1 and 7 days, with a maximum lifetime in the winter and a minimum in the summer. We also note that not all emitted NO_x is necessarily deposited as inorganic TNO_3. The cycling of organic nitrates or formation of reservoir species can extend the effective lifetime of TNO_3 to deposition, as well as lead to additional organic nitrogen deposition that is not captured by the TNO_3 wet deposition measurements (Browne & Cohen, 2012; Fisher et al., 2016).

We used a 'zero CONUS anthropogenic emissions' (noAnthro) simulation for the year 2011 to assess the impact of background (natural + transboundary) emissions and to understand the fractional contribution of CONUS anthropogenic sources of SO_x and TNO_3 on CONUS deposition. The difference between the baseline and the noAnthro simulation allows us to isolate the transport and deposition of CONUS emissions. We note that there are some non-linear effects of zeroing out NO_x emissions on SO_x deposition and *vice versa,* as shown by Ge et al. (2023). This can include changing oxidation rates and thus changing the form of deposition (wet vs. dry). Sensitivity tests where we zero out anthropogenic emissions of NO_x and SO_x independently show these effects to be modest (<10%) in our simulation. Figure 4b shows that in 2011 anthropogenic SO_x contributed up to 90% of all simulated SO_x deposition in the northeastern U.S., downwind of the highest emissions (Figure 2a). The west coast is influenced by both natural (DMS) and transboundary sources (Heald et al., 2006; Park et al., 2004), with anthropogenic SO_x contributing less than 40% to total simulated SO_x deposition, indicating that deposition measurements in these regions are less likely to be representative of the national trends in anthropogenic emissions. Of the total anthropogenic SO_x emitted in CONUS, 70% is deposited in CONUS, and 75% of the SO_x deposited in CONUS come from CONUS anthropogenic emissions. Although the system is not perfectly closed, with some CONUS-origin SO_x removed over neighboring countries and the Atlantic Ocean due to prevailing mid-latitude

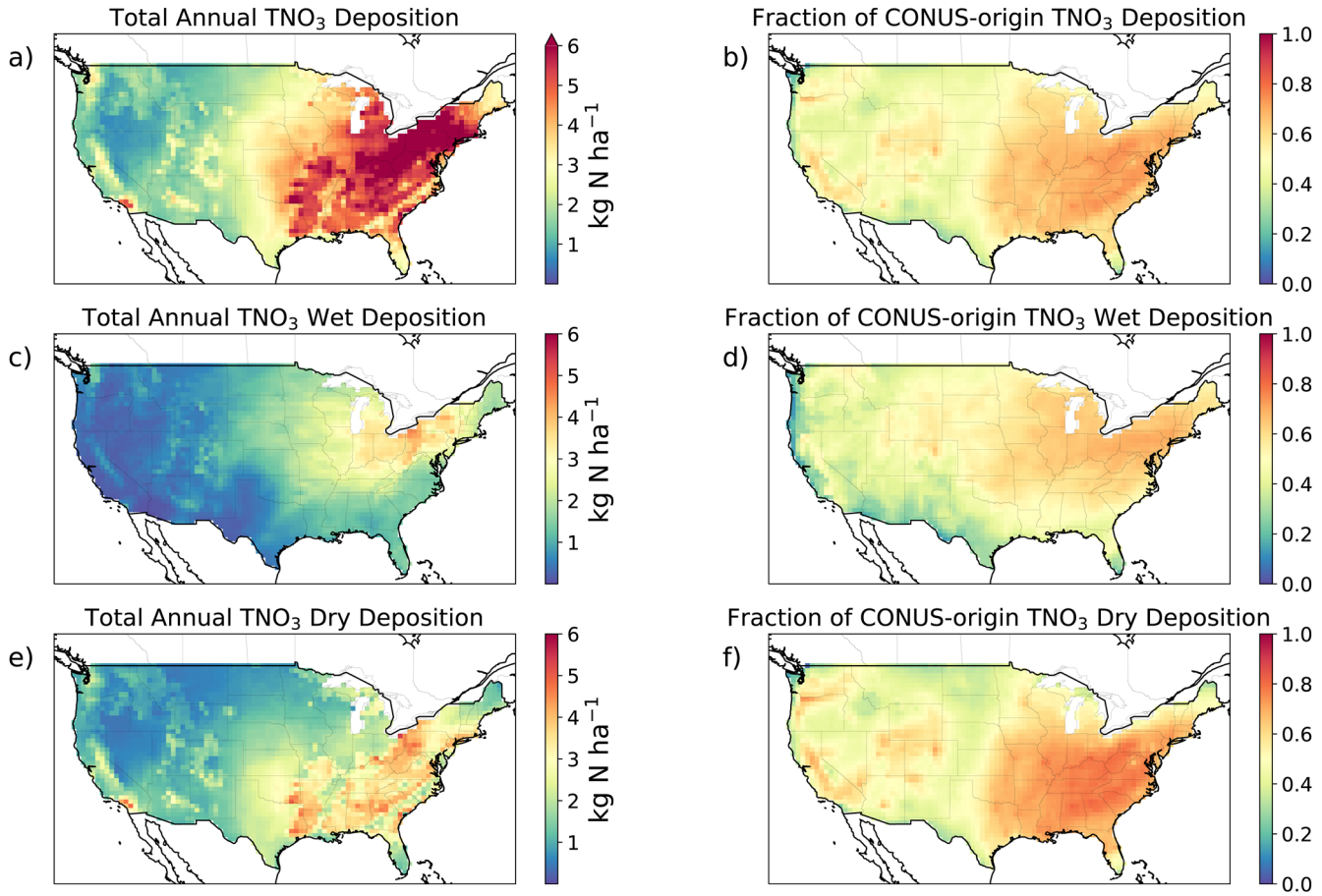

Figure 5. GEOS-Chem simulation of (a) total, (c) wet, and (e) dry annual mean TNO_3 deposition in 2011, and (b, d, f) fractions of simulated TNO_3 deposition originating from conterminous United States (CONUS) anthropogenic sources.

westerlies, a major fraction of CONUS anthropogenic SO_x is deposited domestically. A comparison of Figures 4d and 4f demonstrates that dry deposition reflects a greater proportion of CONUS-origin sources than wet deposition. This reflects that dry deposition is dominated by the freshly emitted gas-phase SO_2, whereas wet deposition is dominated by the oxidized particulate sulfate formed downwind.

Figure 5b shows that, unlike SO_x, which is concentrated in the eastern U.S., CONUS-origin anthropogenic sources make up a large, sometimes dominant, fraction of TNO_3 deposition in the western U.S. (contributing to ~50% of all TNO_3 deposition throughout, with industrial regions and densely populated areas receiving up to ~85%). Despite sources of anthropogenic NO_x being comparatively diffuse in CONUS, approximately 72% is deposited within CONUS as TNO_3, and approximately 69% of TNO_3 deposited in CONUS comes from CONUS anthropogenic sources. These numbers are comparable to those for SO_x deposition, because the clustering of SO_x sources in the Northeast induces greater loss to transport over the Atlantic Ocean. In addition, TNO_3 only accounts for approximately 79% of CONUS anthropogenic NO_y deposition, with the rest being deposited as $orgNO_3$ (in line with estimates made by Ng et al., 2017). As with SO_x, CONUS sources contribute more to dry deposition of TNO_3 than wet deposition (Figures 5d and 5f).

We note that the fractions shown in Figures 4 and 5 represent the 2011 balance between anthropogenic and background sources, and that earlier years exhibit greater anthropogenic influence, and later years exhibit lesser anthropogenic influence.

3.3. Model Evaluation of Deposition

To evaluate model skill in replicating deposition across CONUS, we consider our anchor year (2011) for the evaluation, as it is the native year of the NEI inventory that we use and requires no scaling of emissions estimates.

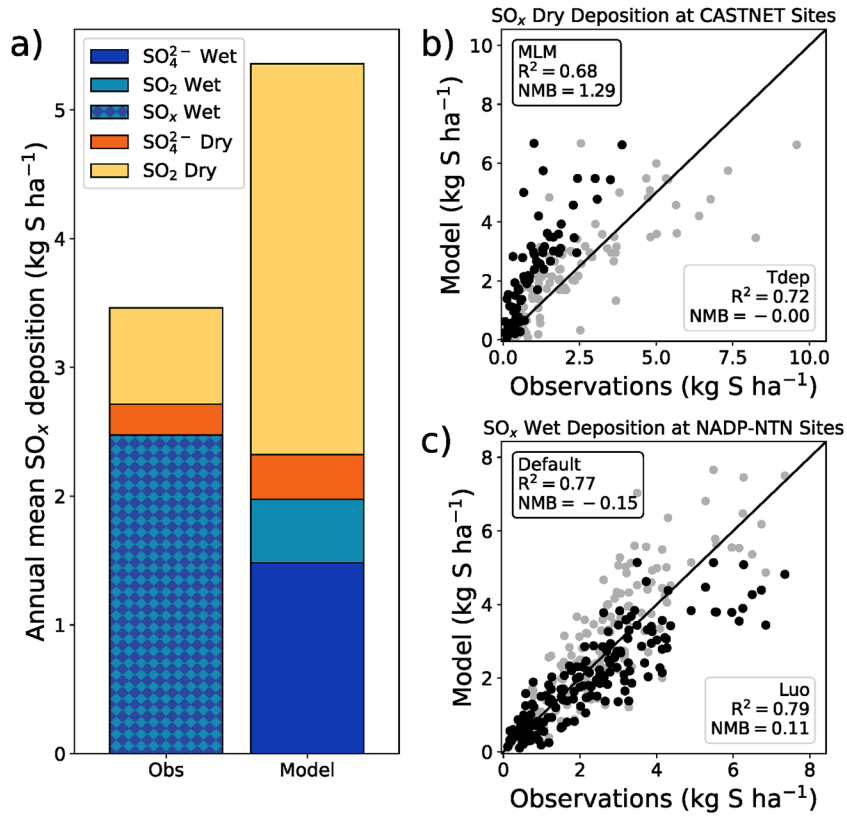

Figure 6. Comparisons between observed and simulated (GEOS-Chem) SO_x deposition for 2011. (a) National annual mean simulated and observed deposition at the National Atmospheric Deposition Program's National Trends Network (NADP-NTN) sites and Clean Air Status and Trends Network (CASTNET) sites, shown by species and deposition mode (b) derived dry deposition fluxes from CASTNET using multi-layer model (MLM) dry deposition velocities (black) and Tdep dry deposition velocities (gray) (c) wet deposition using the default wet deposition scheme (black) and with the Luo updates (gray) in GEOS-Chem. Scatter plot panels include the 1:1 line in black, and summary statistics inset.

3.3.1. Sulfur System

Figure 6 shows annual model-measurement comparisons for SO_x deposition made on a site-wise basis. We see that the annual magnitude and spatial variability of wet deposition is well-represented in the model (annual $R^2 = 0.77$, NMB = −15%). When using the updated wet deposition scheme (shown in gray in Figure 6c), the model shows similar performance with an overestimate rather than underestimate ($R^2 = 0.79$, NMB = 11%).

Figures 6a and 6b show that while the model captures much of the variability in the SO_x dry deposition flux ($R^2 = 0.68$), it substantially overestimates the reported magnitude (NMB = 129%), primarily due to a large overestimate in SO_2 dry deposition flux (which dominates the total dry deposition flux in both model and observations). The bias is highest in the summer and fall (276% and 203%, respectively), and lowest in the winter and spring (123% and 106%, respectively). This overestimate is almost entirely due to a model overestimate of the dry deposition velocity of SO_2. However, as discussed in Section 2.2, an alternate CMAQ-based approach to deriving the dry deposition fluxes at CASTNET sites produces substantially higher values (Schwede & Lear, 2014), and therefore lower bias when compared to GEOS-Chem. Figure 6b shows that we find a much better agreement between the modeled and the network-reported dry SO_x deposition ($R^2 = 0.72$, NMB = 0%) by using these CMAQ-derived fluxes (gray dots). This discrepancy reflects the underlying uncertainty in model-observation comparisons of dry deposition as a derived quantity, arising from varying estimates of dry deposition velocity, and therefore dry deposition fluxes. The long-term analysis envisioned in this work requires the use of the MLM-based dry deposition fluxes (which are available for a longer period than the newer approach) shown in Figure 6a, however, these comparisons suggest that these derived dry deposition fluxes cannot be used to definitively assess the quality of the GEOS-Chem simulation and may not be reliable for assessing long-term trends.

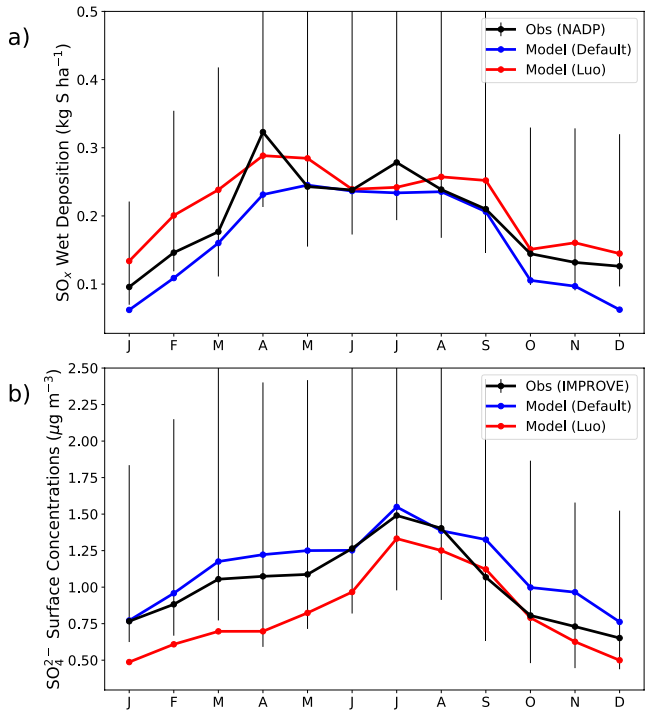

Figure 7. Monthly mean model-observation comparison of (a) wet deposition of sulfate at the National Atmospheric Deposition Program's National Trends Network (NADP-NTN) sites, and (b) ambient surface sulfate concentrations at Interagency Monitoring of Protected Visual Environments (IMPROVE) sites, using both default and Luo wet deposition in GEOS-Chem. Error bars indicate the interquartile range of monthly values across measurement sites.

Figure 7 compares the monthly model-simulated SO_x wet deposition and sulfate concentrations to observations when using either the standard or the Luo et al. (2019, 2020) updates to the wet deposition scheme. The Luo updates cause a substantial increase in wintertime SO_2 wet deposition in addition to a more moderate increase in SO_4^{2-} wet deposition which decreases SO_x lifetimes in the winter compared to the default deposition scheme. There is also a corresponding decrease in dry deposition, leading to a slight reduction in the high bias ($R^2 = 0.57$, NMB = 82%), but the increase in wet deposition dominates, with a net increase in total SO_x deposition shown in Figure 7a. As shown in Figure 6c, both schemes are similarly modestly biased compared to observed wet deposition (standard scheme too low, Luo scheme too high). As expected with such an increase in SO_x deposition, the Luo et al. updates reduce ambient sulfate concentrations in the model. While the Luo scheme eliminates the slight high bias at Interagency Monitoring of Protected Visual Environment (IMPROVE) sites in the fall, the increase in deposition results in a low bias in simulated sulfate concentrations through the rest of the year (NMB changes from 11% with the default scheme to −20% with the Luo scheme) (Figure 7b). The generally good simulation of both sulfate concentrations and SO_x wet removal in the standard model do not support a substantial bias in dry deposition suggested by our comparisons in Figure 6a. This further indicates that the MLM-based CASTNET observations that we use here (shown in Figure 6) are biased low.

Given the variability in SO_x emissions and deposition across the United States (Figures 2 and 4a), we investigate the model's spatial representation of SO_x deposition. For this more granular assessment, we aggregate sites by EPA region and compare the wet annual SO_x deposition (Figure 8). Given the uncertainty in observed dry deposition described above, the spatial dry deposition comparisons are shown in SI (Figure S2 in Supporting Information S1). We also show in Figure 8 the number of measurement sites in each region, ranging from 7 to 36 sites, indicating that some regions (e.g. EPA Regions 4, 5, 8) may be better characterized by these regional averages than others. As a means of assessing the representativeness of these sites of the regional average, we include in Figure 8 the average of all the model gridboxes in each region (not just sampled at the measurement sites). We take good agreement between the

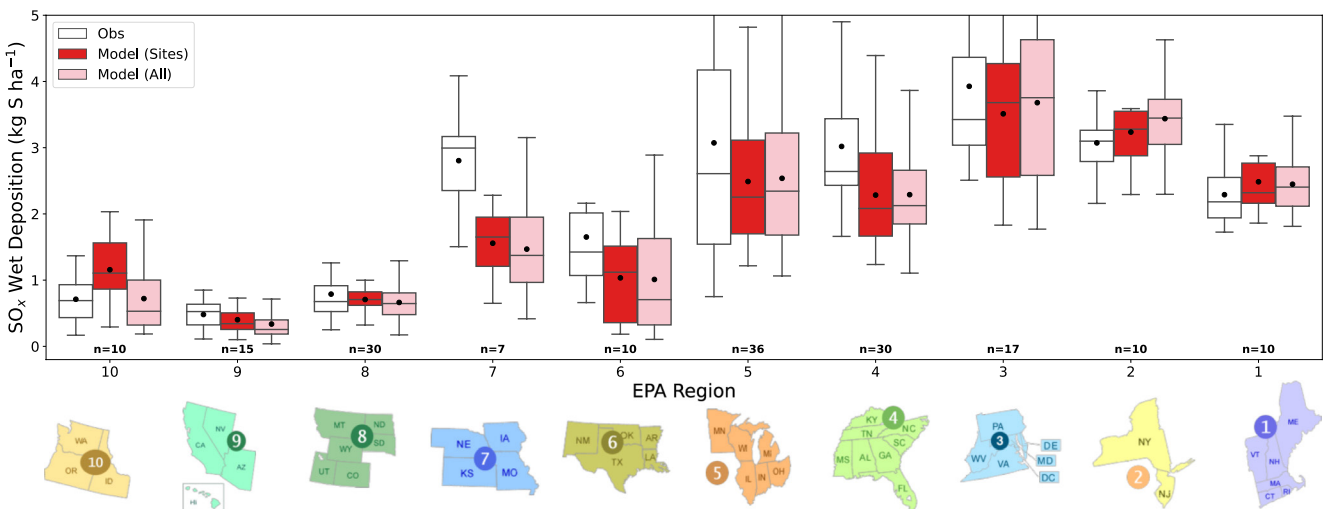

Figure 8. Model-observation comparison for wet SO_x deposition in 2011, aggregated by Environmental Protection Agency (EPA) regions (illustrated below bar plot), arranged approximately west to east. Boxes show the median and interquartile range of mean annual deposition across all sites in a given EPA region, and black points show the regional annual mean. The distribution of the observations within each region (white) is compared with the model sampled at these sites (red) as well as all the model gridboxes within each region (pink). The number of sites in each region are noted below each group of boxes.

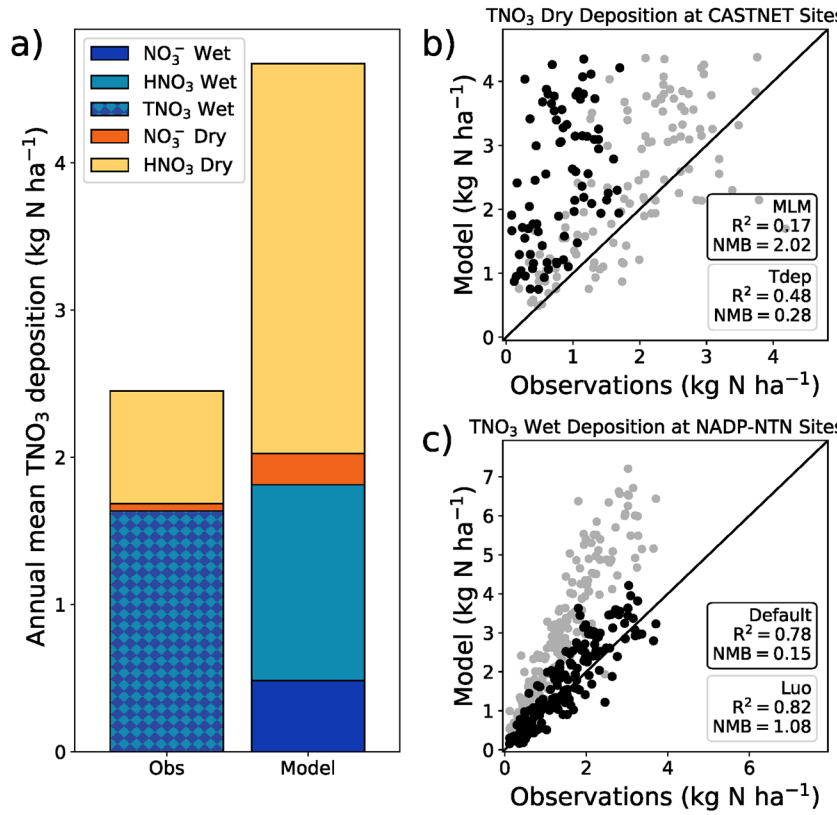

Figure 9. Comparison between observed and simulated (GEOS-Chem) TNO_3 deposition for 2011. (a) National annual mean simulated and observed deposition at the National Atmospheric Deposition Program's National Trends Network (NADP-NTN) and Clean Air Status and Trends Network (CASTNET) sites, shown by species and deposition mode, (b) dry deposition from CASTNET using multi-layer model (MLM) dry deposition velocities (black) and Tdep dry deposition velocities (gray) (c) wet deposition using the default wet deposition scheme (black) and with the Luo updates (gray) in GEOS-Chem. Scatter plot panels include the 1:1 line in black, and summary statistics inset.

model sampled at the sites compared to the model averaged over the entire region as indicative of good site representativeness.

The spatial pattern of deposition generally follows emissions and the associated transport downwind by prevalent westerly winds. Much of the West Coast (Regions 9 and 10) is dominated by background SO_x sources (Figure 4b), with low SO_x deposition. The comparison in Figure 8 suggests that these background sources are well represented in the GEOS-Chem model. There is a noticeable jump in deposition in the industrial Midwest (Region 5), the Southeast (Region 4), and the coal-producing mid-Atlantic (Region 3), and the model shows a slight low bias in these regions. Although SO_x emissions are relatively low in much of the Northeast, we still see elevated wet deposition relative to the Western U.S. due to transport from emissions upwind. Except for Regions 9 and 10, the regional means sampled at the sites and across all gridboxes are within 7%. While wet deposition measurement sites in Regions 9 and 10 (Southwest and Pacific Northwest) are least representative of the region at large (differences of 19% and 60%, respectively), both regions have some of the lowest SO_x emissions and deposition in the country. This comparison suggests that there are no substantial or systematic representation errors in wet deposition with the NADP-NTN measurement network for the purposes of comparison with the model in 2011.

3.3.2. Total Nitrate System

Figure 9 compares simulated and measured TNO_3 deposition at CASTNET and NADP-NTN sites. The standard model captures the spatial variability in wet deposition with a slight high bias ($R^2 = 0.78$, NMB = 15%). The Luo et al. scheme (gray dots in Figure 9c) results in a substantial overestimate of observed TNO_3 wet deposition at NADP-NTN sites ($R^2 = 0.82$, NMB = 108%). Much of this bias is attributable to overestimated wet nitric acid deposition (simulated HNO_3 wet deposition alone exceeds the observed TNO_3 wet

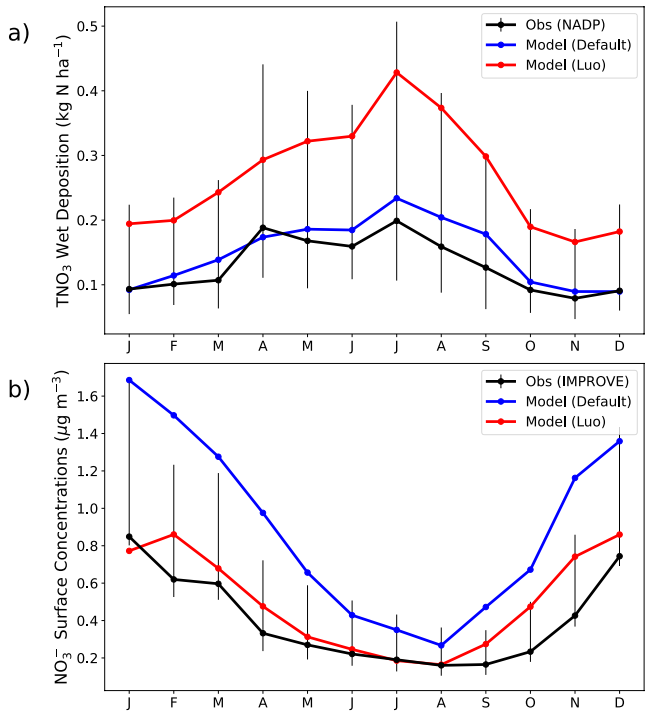

Figure 10. Monthly mean model-observation comparison of (a) wet-deposited nitrate at the National Atmospheric Deposition Program's National Trends Network sites (NADP-NTN), and (b) ambient surface nitrate concentrations at Interagency Monitoring of Protected Visual Environments (IMPROVE) sites, using both default and Luo wet deposition in GEOS-Chem. Error bars indicate the interquartile range of monthly values across measurement sites.

deposition), which is the result of the significantly higher nitric acid washout rate implemented by Luo et al. (2019). As is the case with SO_x dry deposition, comparisons with the MLM-derived deposition (black dots in Figure 9b) are substantially high-biased (R^2 = 0.17, NMB = 202%). This high bias is driven by high-biased HNO_3 dry deposition, which is largely due to a model overestimate of the dry deposition velocity of HNO_3. The model agrees better with CMAQ-derived Tdep dry deposition for TNO_3 (R^2 = 0.48, NMB = 28%). As with SO_x, given the ambiguity in observed dry deposition of TNO_3, we focus primarily on wet deposition in the following discussion.

Figure 10a demonstrates that TNO_3 wet deposition is well-captured year-round in the standard model, and that this comparison is substantially degraded with the Luo et al. scheme. However, Figure 10b also shows that the standard model substantially overestimates NO_3^- concentrations observed at IMPROVE sites (NMB = 121%), as seen in previous studies (Heald et al., 2012; Walker et al., 2012). L. Zhang et al. (2012) showed similar behavior over the United States, with a high nitrate concentration bias and an unbiased simulation of TNO_3 wet deposition in a previous version of the GEOS-Chem model. The bias in simulated nitrate concentrations is virtually eliminated (NMB = 23%) by including the Luo et al. wet deposition updates (Figure 10b). Therefore, we find that with or without the updated wet deposition scheme, the model cannot simultaneously meet the observational constraints on nitrate concentrations and TNO_3 deposition. Previous work by Travis et al. (2016), suggested that NEI 2011 may overestimate NO_x mobile sources in the United States by ~60%. We conducted a pair of sensitivity tests in 2011 by reducing anthropogenic NO_x emissions in CONUS by 30% and 50%, and found that although surface NO_x reduced almost uniformly across CONUS (commensurate with the reduction in emissions) the magnitude and sign of the changes in NO_3^- concentrations varied regionally depending on the chemical environment and the impacts of NO_x emissions changes on local oxidants. This suggests that the model biases in the simulation of the TNO_3 system cannot simply be explained as a large overestimate of NO_x emissions.

We further note that while the Luo et al. (2020) scheme produces a generally unbiased simulation of nitrate concentrations over the United States, Travis et al. (2022) find that the inclusion of the Luo et al. (2019) update was insufficient to address the overestimate of atmospheric nitrate over Korea during KORUS-AQ. They invoked a five-fold increase in the dry depositional sink of HNO_3 associated with uptake on urban surfaces to address the nitrate concentration bias over Korea. However, such an increase associated with urban conditions would not be relevant to the entirety of the United States, and our comparisons do not support such a large increase in modeled HNO_3 dry deposition (which is already overestimated compared to either set of CASTNET dry deposition data sets). Together, previous work and our results indicate that there remain considerable uncertainties in the simulation of nitrate that may vary by region around the globe.

As with SO_x, we investigate the model's spatial representation of TNO_3 deposition. NO_x emissions and deposition are even more spatially dispersed than SO_x emissions (Figures 2 and 5). Figures 5 and 11 show that TNO_3 deposition is high throughout much of the central and eastern U.S., reflecting the greater western extent of CONUS anthropogenic NO_x emissions compared to SO_x (Figure 2b), but nonetheless is subject to similar westerly transport and transboundary loss. The model is biased high near the Great Lakes (Region 5), and in the Northeast and Mid-Atlantic (Regions 1, 2, and 3) (all regions with high NO_x emissions, and therefore high TNO_3 deposition) (Figure 11). Regions in the North (1, 2, 3, 5, and 7) have greater TNO_3 wet deposition compared to the South and Southeast (Regions 4 and 6), which are more influenced by dry deposition (Figure 5). As seen with SO_x, the simulated average over a region compares well with the average sampled only at measurement sites within each region. Barring Region 10, which experiences relatively low annual TNO_3 deposition, the two regional means are within 8% of each other, suggesting that the NADP-NTN measurement networks again provide enough spatial coverage to adequately represent each EPA region for the year 2011.

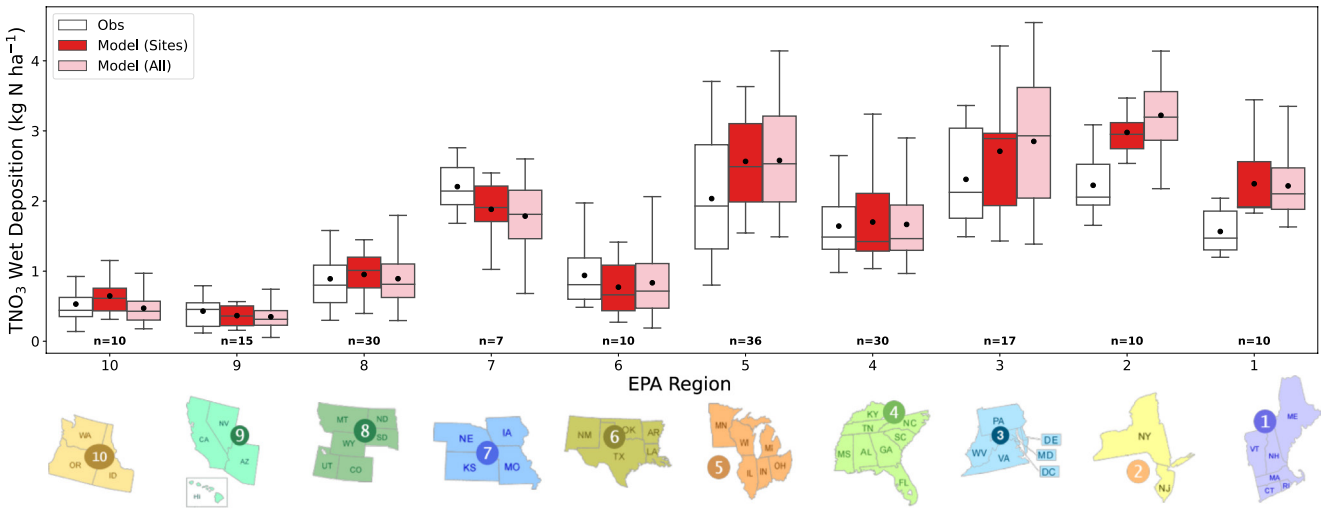

Figure 11. Model-observation comparison for wet TNO_3 deposition in 2011, aggregated by Environmental Protection Agency (EPA) regions (illustrated below bar plot), arranged approximately west to east. Boxes show the median and interquartile range of mean annual deposition across all sites in a given EPA region, and black points show the regional annual mean. The distribution of the observations within each region (white) is compared with the model sampled at these sites (red) as well as all the model gridboxes within each region (pink). The number of sites in each region is noted below each group of boxes.

3.4. Trends in Deposition and Anthropogenic Emissions

While uncertainties in dry deposition observations challenge our ability to evaluate total deposition, in Section 3.3 we find that the standard GEOS-Chem model is able to reasonably capture the observed magnitude and spatial distribution of wet deposition of SO_x and TNO_3 for a year in which emissions are well-constrained. Additionally, we find that the high model bias in SO_x and TNO_3 dry deposition is consistent over time (Figure S3 in Supporting Information S1), and we note that there is no discernible trend in either the simulated or "observed" MLM dry deposition velocities for SO_2, HNO_3, or particulates. Therefore, any trends in dry deposition are almost entirely attributable to the trends in measured concentrations. Given that dry deposition is dominated by primary, gas-phase species (SO_2 and HNO_3) and not secondary particulates, we expect these trends in concentrations to follow trends in emissions to first order. The consistency of these biases also suggests that the relative trends in emissions and deposition may be consistent for both SO_x and TNO_3. We therefore explore the relationship between emissions and deposition over several decades. To ensure consistency, we use the NEI 2011 anthropogenic emission inventory scaled state-wise (Figure S1 in Supporting Information S1); the uncertainty in the emissions estimates therefore likely increases as we move further away from the anchor year of 2011. However, anthropogenic SO_2 emissions in CONUS are dominated by monitored EGU point sources, and therefore these emissions over time should be well-constrained.

Figure 12a shows that the model (driven by scaled NEI 2011 emissions) is skilled at representing the relative trends in SO_x wet and dry deposition since 1990. We see that the relative trend in observed and modeled dry deposition (yellow line and symbols) closely follows the trend in anthropogenic SO_2 emissions (dashed red line) from 1990 to 2021. This is consistent with Figure 4 which shows that SO_x dry deposition (which is dominated by freshly emitted SO_2, as shown in Figure 6) in the United States is relatively local and highly influenced by anthropogenic emissions. Observed (modeled) dry deposition and anthropogenic emissions of SO_x decrease by 93% (94%) and 93%, respectively during this time period. The decline in observed (simulated) wet deposition of SO_x (blue line and symbols) is slightly more modest 78% (79%). Ge et al. (2023) show that, in North America, both SO_2 and sulfate respond linearly to cuts in SO_x emissions. This too is consistent with Figure 4 which shows that wet-deposited SO_x (which is dominated by sulfate, as shown in Figure 6) is more strongly influenced by background (including transboundary and natural) sources which moderate the sharp decline in CONUS anthropogenic emissions. Figure 12a suggests that there is an opportunity to use these consistent, long-term, spatially-heterogeneous derived SO_x dry deposition observations to estimate changing anthropogenic SO_x emissions over time.

Figure 12b provides similar insight into the TNO_3 system. The model captures the relative trend in observed dry (yellow) and wet (blue) deposition. Anthropogenic NO_x emissions in the United States started to substantially

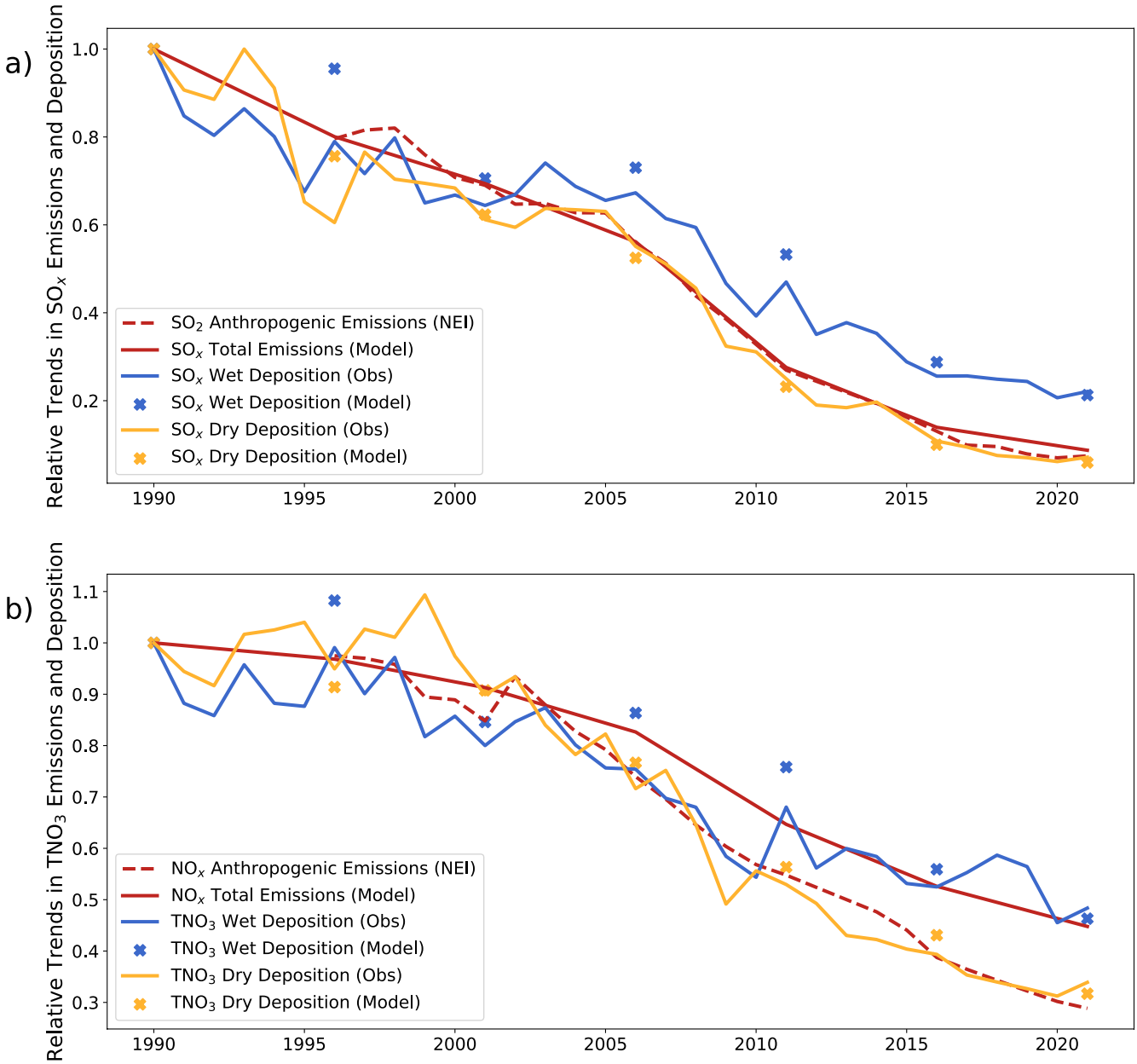

Figure 12. Trends in emissions and mean annual deposition (modeled and measured) for (a) SO_x and (b) TNO_3 relative to 1990. Annual anthropogenic emissions (dashed red line) are from the National Emissions Inventory (NEI), total (anthropogenic + natural) emissions (solid red line) are calculated using model output for simulated years. Modeled wet deposition (blue crosses) agrees well with measurements (blue line), and modeled dry deposition (yellow crosses) agrees well with measured dry deposition (yellow line).

decline in the early 2000s, thereby increasing the importance of natural and transboundary sources of TNO_3, which remained relatively constant. Figure 12b demonstrates this divergence in the trend in total and anthropogenic NO_x emissions. Table 1 shows how natural NO_x sources contributed only 13% of the total in 1990, but increased to 42% by 2021. The observed (simulated) dry deposition (yellow line and symbols), decreases by 66% (68%), closely tracking the 71% decline in anthropogenic emissions (dashed red line) between 1990 and 2021, and congruent with findings from the noAnthro simulation, in which dry deposition strongly reflects local anthropogenic sources (Figure 5f). The observed (simulated) trend in TNO_3 wet deposition (blue line and symbols), a 52% (54%) decrease from 1990 to 2021, is closely aligned with the decrease in total NO_x emissions in the United States (solid red line) (55% from 1990 to 2021). Silvern et al. (2019) similarly note that the trends in total NO_2 column and TNO_3 wet deposition over the United States reflect trends in total NO_x sources, while Benish

et al. (2022) note the recent steeper decline in oxidized nitrogen dry deposition compared to that of wet deposition. This suggests that while TNO_3 wet deposition measurements may have provided a valuable constraint on anthropogenic emissions in CONUS in the past, the measurements increasingly reflect trends in natural sources. Similar to the SO_x system, the relative trend in observed dry deposition appears to be a better constraint on US anthropogenic sources.

4. Conclusions

Accurately characterizing trends in anthropogenic emissions is critical to verifying the effectiveness of air quality policies. However, estimating emissions trends comes with numerous challenges, including a lack of spatial or temporal coverage in measurement methods and changes in underlying modeling frameworks. In this study, we explored whether long-running, spatially-heterogeneous measurements made at deposition networks in the United States provide a constraint on emissions trends of SO_x and NO_x between 1990 and 2021.

We use GEOS-Chem as an intermediary between deposition measurements and emissions inventories. Therefore, we first evaluate the GEOS-Chem simulation of deposition for the SO_x and TNO_3 system in the United States. SO_x and TNO_3 wet deposition are well-represented in the model. We find that an updated wet deposition scheme by Luo et al. (2019, 2020) rectifies the overestimate in surface NO_3^- concentrations at the expense of TNO_3 wet deposition, significantly degrading model performance as a result of a large increase in HNO_3 wet removal. Our analysis of simultaneous concentration and deposition measurements illustrates a long-standing issue that the model cannot simultaneously provide an unbiased simulation of both, suggesting additional unidentified sinks of NO_y. An evaluation of the model's representation of dry deposition is challenging given the two drastically different available estimates from CASTNET. When evaluated against the legacy measurements which use deposition velocities derived from an MLM, model performance is poor for both the SO_x and TNO_3 systems. Comparison against more recently derived measurements, which use higher CMAQ-derived deposition velocities for both species, demonstrates little model bias in SO_x and TNO_3 dry deposition. However, these CMAQ-derived deposition velocities do not extend over the entire time period of interest for this study. This comparison points to the substantial uncertainty surrounding the dry deposition velocity used to estimate CASTNET dry deposition fluxes.

While there is a large range of uncertainty in model-derived dry deposition measurements, we have shown that the GEOS-Chem model captures the relative trend in both wet and dry SO_x and TNO_3 deposition in CONUS between 1990 and 2021, and that the relative trends in dry deposition capture the relative trend in anthropogenic SO_2 and NO_x emissions over CONUS in the same period. While dry deposition strongly reflects local CONUS anthropogenic emissions, wet deposition observations are more impacted by natural and transboundary sources. Thus, for both the SO_x and TNO_3 systems, the wet deposition trend is moderated by more consistent background sources. We therefore find that the dry deposition measurements may provide a better constraint on trends in anthropogenic CONUS SO_x and NO_x emissions, while wet deposition measurements reflect the trend in all SO_x and TNO_3 sources impacting the United States.

Deposition measurements of SO_x and TNO_3 provide a vital observational basis to evaluate model skill in representing the SO_x and TNO_3 systems over time. Our analysis shows that these long-term, continuous observations can provide a useful constraint on sources in the United States. This indicates that routine deposition network measurements may be used to develop interim emission inventory updates at the national scale, for example, scaling a bottom-up emissions inventory to a more recent year based on a comparison of observed deposition. Furthermore, it may be possible to estimate trends in regional emissions, as well as disaggregate anthropogenic and background sources, from deposition data by using an inverse modeling framework. This work also underscores the critical uncertainties in derived dry deposition measurements, with different models leading to a wide range of possible deposition velocities. This highlights the need for the evaluation (e.g., against eddy covariance observations) and advancement of schemes to derive local dry deposition velocities.

Data Availability Statement

The data that support the findings of this study are available on Zenodo (Dutta & Heald, 2023). The GEOS-Chem model is publicly available (GEOS-Chem v13.3.4, 2021). The NADP-NTN data are available publicly (NADP, 2022) (last access: 20 July 2022). The CASTNET data are available publicly (CASTNET, 2022) (last

access: 6 September 2022). The IMPROVE data are available publicly (IMPROVE, 2022) (last access: 26 September 2022).

Acknowledgments
This study was supported by the NOAA Climate Program Office (Grant NA19OAR4310180). ID was partially supported by a Callahan-Dee fellowship. We would like to acknowledge the Clean Air Status and Trends Network (CASTNET), the Interagency Monitoring of Protected Visual Environments (IMPROVE), and the National Trends Network (NTN) for measurement data used in this work.

References

Amos, H. M., Jacob, D. J., Holmes, C. D., Fisher, J. A., Wang, Q., Yantosca, R. M., et al. (2012). Gas-particle partitioning of atmospheric Hg(II) and its effect on global mercury deposition. *Atmospheric Chemistry and Physics*, *12*(1), 591–603. https://doi.org/10.5194/acp-12-591-2012

Bates, K. H., & Jacob, D. J. (2019). A new model mechanism for atmospheric oxidation of isoprene: Global effects on oxidants, nitrogen oxides, organic products, and secondary organic aerosol. *Atmospheric Chemistry and Physics*, *19*(14), 9613–9640. https://doi.org/10.5194/acp-19-9613-2019

Bell, M. L., Dominici, F., Ebisu, K., Zeger, S. L., & Samet, J. M. (2007). Spatial and temporal variation in $PM_{2.5}$ chemical composition in the United States for health effects studies. *Environmental Health Perspectives*, *115*(7), 989–995. https://doi.org/10.1289/ehp.9621

Benish, S. E., Bash, J. O., Foley, K. M., Appel, K. W., Hogrefe, C., Gilliam, R., & Pouliot, G. (2022). Long-term regional trends of nitrogen and sulfur deposition in the United States from 2002 to 2017. *Atmospheric Chemistry and Physics*, *22*(19), 12749–12767. https://doi.org/10.5194/acp-22-12749-2022

Bouwman, A. F., Van Vuuren, D. P., Derwent, R. G., & Posch, M. (2002). A global analysis of acidification and eutrophication of terrestrial ecosystems. *Water, Air, and Soil Pollution*, *141*(1), 349–382. https://doi.org/10.1023/A:1021398008726

Bowker, G. E., Schwede, D. B., Lear, G. G., Warren-Hicks, W. J., & Finkelstein, P. L. (2011). Quality assurance decisions with air models: A case study of imputation of missing input data using EPA's multi-layer model. *Water, Air, & Soil Pollution*, *222*(1), 391–402. https://doi.org/10.1007/s11270-011-0832-7

Browne, E. C., & Cohen, R. C. (2012). Effects of biogenic nitrate chemistry on the NO_x lifetime in remote continental regions. *Atmospheric Chemistry and Physics*, *12*(24), 11917–11932. https://doi.org/10.5194/acp-12-11917-2012

Butler, T. J., Likens, G. E., & Stunder, B. J. B. (2001). Regional-scale impacts of Phase I of the Clean Air Act Amendments in the USA: The relation between emissions and concentrations, both wet and dry. *Atmospheric Environment*, *35*(6), 1015–1028. https://doi.org/10.1016/S1352-2310(00)00386-1

Butler, T. J., Likens, G. E., Vermeylen, F. M., & Stunder, B. J. B. (2003). The relation between NO_x emissions and precipitation NO_3^- in the eastern USA. *Atmospheric Environment*, *37*(15), 2093–2104. https://doi.org/10.1016/S1352-2310(03)00103-1

CASTNET. (2020). *Clean Air Status and Trends Network Quality Assurance Project Plan*. United States Environmental Protection Agency. Retrieved from https://www3.epa.gov/castnet/docs/CASTNET_QAPP_v9-4_Main_Body_Final.pdf

CASTNET. (2022). US EPA Clean Air Markets Division: Dry Deposition Weekly (Web) Report [Dataset]. Retrieved from http://www.epa.gov/castnet

Dockery, D. W., Pope, C. A., Xu, X., Spengler, J. D., Ware, J. H., Fay, M. E., et al. (1993). An association between air pollution and mortality in six U.S. cities. *New England Journal of Medicine*, *329*(24), 1753–1759. https://doi.org/10.1056/NEJM199312093292401

Dutta, I., & Heald, C. L. (2023). Exploring deposition observations of oxidized sulfur and nitrogen as a constraint on emissions in the United States [Dataset]. https://doi.org/10.5281/zenodo.8099927

Emerson, E. W., Hodshire, A. L., DeBolt, H. M., Bilsback, K. R., Pierce, J. R., McMeeking, G. R., & Farmer, D. K. (2020). Revisiting particle dry deposition and its role in radiative effect estimates. *Proceedings of the National Academy of Sciences*, *117*(42), 26076–26082. https://doi.org/10.1073/pnas.2014761117

Fairlie, T. D., Jacob, D. J., & Park, R. J. (2007). The impact of transpacific transport of mineral dust in the United States. *Atmospheric Environment*, *41*(6), 1251–1266. https://doi.org/10.1016/j.atmosenv.2006.09.048

Finkelstein, P. L., Ellestad, T. G., Clarke, J. F., Meyers, T. P., Schwede, D. B., Hebert, E. O., & Neal, J. A. (2000). Ozone and sulfur dioxide dry deposition to forests: Observations and model evaluation. *Journal of Geophysical Research: Atmospheres*, *105*(D12), 15365–15377. https://doi.org/10.1029/2000JD900185

Fisher, J. A., Jacob, D. J., Travis, K. R., Kim, P. S., Marais, E. A., Chan Miller, C., et al. (2016). Organic nitrate chemistry and its implications for nitrogen budgets in an isoprene- and monoterpene-rich atmosphere: Constraints from aircraft (SEAC^{4}RS) and ground-based (SOAS) observations in the Southeast US. *Atmospheric Chemistry and Physics*, *16*(9), 5969–5991. https://doi.org/10.5194/acp-16-5969-2016

Foley, K. M., Pouliot, G. A., Eyth, A., Aldridge, M. F., Allen, C., Appel, K. W., et al. (2023). 2002–2017 anthropogenic emissions data for air quality modeling over the United States. *Data in Brief*, *47*, 109022. https://doi.org/10.1016/j.dib.2023.109022

Fountoukis, C., & Nenes, A. (2007). ISORROPIA II: A computationally efficient thermodynamic equilibrium model for K^+–Ca^{2+}–Mg^{2+}–NH_4^+–Na^+–SO_4^{2-}–NO_3^-–Cl^-–H_2O aerosols. *Atmospheric Chemistry and Physics*, *7*(17), 4639–4659. https://doi.org/10.5194/acp-7-4639-2007

Freese, L. M., Chossière, G. P., Eastham, S. D., Jenn, A., & Selin, N. E. (2023). Nuclear power generation phase-outs redistribute US air quality and climate-related mortality risk. *Nature Energy*, *8*(5), 492–503. https://doi.org/10.1038/s41560-023-01241-8

Ge, Y., Vieno, M., Stevenson, D. S., Wind, P., & Heal, M. R. (2023). Global sensitivities of reactive N and S gas and particle concentrations and deposition to precursor emissions reductions. *Atmospheric Chemistry and Physics*, *23*(11), 6083–6112. https://doi.org/10.5194/acp-23-6083-2023

GEOS-Chem v13.3.4. (2021). https://doi.org/10.5281/zenodo.5764874

Gilliland, A. B., Appel, K. W., Pinder, R. W., & Dennis, R. L. (2006). Seasonal NH3 emissions for the continental United States: Inverse model estimation and evaluation. *Atmospheric Environment*, *40*(26), 4986–4998. https://doi.org/10.1016/j.atmosenv.2005.12.066

Gilliland, A. B., Dennis, R. L., Roselle, S. J., & Pierce, T. E. (2003). Seasonal NH3 emission estimates for the eastern United States based on ammonium wet concentrations and an inverse modeling method. *Journal of Geophysical Research: Atmospheres*, *108*(D15). https://doi.org/10.1029/2002JD003063

Guenther, A. B., Jiang, X., Heald, C. L., Sakulyanontvittaya, T., Duhl, T., Emmons, L. K., & Wang, X. (2012). The Model of Emissions of Gases and Aerosols from Nature version 2.1 (MEGAN2.1): An extended and updated framework for modeling biogenic emissions. *Geoscientific Model Development*, *5*(6), 1471–1492. https://doi.org/10.5194/gmd-5-1471-2012

Haagen-Smit, A. J. (1952). Chemistry and physiology of Los Angeles Smog. *Industrial & Engineering Chemistry*, *44*(6), 1342–1346. https://doi.org/10.1021/ie50510a045

Hattori, S., Iizuka, Y., Alexander, B., Ishino, S., Fujita, K., Zhai, S., et al. (2021). Isotopic evidence for acidity-driven enhancement of sulfate formation after SO_2 emission control. *Science Advances*, *7*(19), eabd4610. https://doi.org/10.1126/sciadv.abd4610

Heald, C. L., Collett, J. L. J., Lee, T., Benedict, K. B., Schwandner, F. M., Li, Y., et al. (2012). Atmospheric ammonia and particulate inorganic nitrogen over the United States. *Atmospheric Chemistry and Physics*, *12*(21), 10295–10312. https://doi.org/10.5194/acp-12-10295-2012

Heald, C. L., Jacob, D. J., Park, R. J., Alexander, B., Fairlie, T. D., Yantosca, R. M., & Chu, D. A. (2006). Transpacific transport of Asian anthropogenic aerosols and its impact on surface air quality in the United States. *Journal of Geophysical Research: Atmospheres*, *111*(D14). https://doi.org/10.1029/2005JD006847

Henderson, B. H., & Freese, L. M. (2021). Preparation of GEOS-Chem emissions from CMAQ. https://doi.org/10.5281/zenodo.5122827

Hoesly, R. M., Smith, S. J., Feng, L., Klimont, Z., Janssens-Maenhout, G., Pitkanen, T., et al. (2018). Historical (1750–2014) anthropogenic emissions of reactive gases and aerosols from the Community Emissions Data System (CEDS). *Geoscientific Model Development*, *11*(1), 369–408. https://doi.org/10.5194/gmd-11-369-2018

Hu, L., Millet, D. B., Baasandorj, M., Griffis, T. J., Turner, P., Helmig, D., et al. (2015). Isoprene emissions and impacts over an ecological transition region in the U.S. Upper Midwest inferred from tall tower measurements. *Journal of Geophysical Research: Atmospheres*, *120*(8), 3553–3571. https://doi.org/10.1002/2014JD022732

Hudman, R. C., Moore, N. E., Mebust, A. K., Martin, R. V., Russell, A. R., Valin, L. C., & Cohen, R. C. (2012). Steps towards a mechanistic model of global soil nitric oxide emissions: Implementation and space based-constraints. *Atmospheric Chemistry and Physics*, *12*(16), 7779–7795. https://doi.org/10.5194/acp-12-7779-2012

IMPROVE. (2022). Interagency Monitoring of Protected Visual Environments [Dataset]. Boulder, CO: Colorado State University. Retrieved from http://vista.cira.colostate.edu/Improve/

Janssens-Maenhout, G., Crippa, M., Guizzardi, D., Muntean, M., & Schaaf, E. (2011). Emissions database for global atmospheric research. Version v4.2 (time-series). Retrieved from http://data.europa.eu/89h/jrc-edgar-emissiontimeseriesv42

Kim, P. S., Jacob, D. J., Fisher, J. A., Travis, K., Yu, K., Zhu, L., et al. (2015). Sources, seasonality, and trends of southeast US aerosol: An integrated analysis of surface, aircraft, and satellite observations with the GEOS-Chem chemical transport model. *Atmospheric Chemistry and Physics*, *15*(18), 10411–10433. https://doi.org/10.5194/acp-15-10411-2015

Likens, G. E., & Bormann, F. H. (1974). Acid rain: A serious regional environmental problem. *Science*, *184*(4142), 1176–1179. https://doi.org/10.1126/science.184.4142.1176

Liu, H., Jacob, D. J., Bey, I., & Yantosca, R. M. (2001). Constraints from ^{210}Pb and ^{7}Be on wet deposition and transport in a global three-dimensional chemical tracer model driven by assimilated meteorological fields. *Journal of Geophysical Research: Atmospheres*, *106*(D11), 12109–12128. https://doi.org/10.1029/2000JD900839

Luo, G., Yu, F., & Moch, J. M. (2020). Further improvement of wet process treatments in GEOS-Chem v12.6.0: Impact on global distributions of aerosols and aerosol precursors. *Geoscientific Model Development*, *13*(6), 2879–2903. https://doi.org/10.5194/gmd-13-2879-2020

Luo, G., Yu, F., & Schwab, J. (2019). Revised treatment of wet scavenging processes dramatically improves GEOS-Chem 12.0.0 simulations of surface nitric acid, nitrate, and ammonium over the United States. *Geoscientific Model Development*, *12*(8), 3439–3447. https://doi.org/10.5194/gmd-12-3439-2019

McDuffie, E. E., Smith, S. J., O'Rourke, P., Tibrewal, K., Venkataraman, C., Marais, E. A., et al. (2020). A global anthropogenic emission inventory of atmospheric pollutants from sector- and fuel-specific sources (1970–2017): An application of the Community Emissions Data System (CEDS). *Earth System Science Data*, *12*(4), 3413–3442. https://doi.org/10.5194/essd-12-3413-2020

Meyers, T. P., Finkelstein, P., Clarke, J., Ellestad, T. G., & Sims, P. F. (1998). A multilayer model for inferring dry deposition using standard meteorological measurements. *Journal of Geophysical Research: Atmospheres*, *103*(D17), 22645–22661. https://doi.org/10.1029/98JD01564

Murray, C. J. L., Aravkin, A. Y., Zheng, P., Abbafati, C., Abbas, K. M., Abbasi-Kangevari, M., et al. (2020). Global burden of 87 risk factors in 204 countries and territories, 1990–2019: A systematic analysis for the Global Burden of Disease Study 2019. *The Lancet*, *396*(10258), 1223–1249. https://doi.org/10.1016/S0140-6736(20)30752-2

Murray, L. T., Jacob, D. J., Logan, J. A., Hudman, R. C., & Koshak, W. J. (2012). Optimized regional and interannual variability of lightning in a global chemical transport model constrained by LIS/OTD satellite data. *Journal of Geophysical Research: Atmospheres*, *117*(D20). https://doi.org/10.1029/2012JD017934

NADP. (2021a). *2020 Quality Assurance Report*. Central Analytical Laboratory. Madison, WI: National Atmospheric Deposition Program. Retrieved from https://nadp.slh.wisc.edu/quality-assurance/

NADP. (2021b). *NADP/NTN DATA Validation and Completeness Criteria*. National Atmospheric Deposition Program. Retrieved from https://nadp.slh.wisc.edu/networks/national-trends-network/

NADP. (2022). National Trends Network Weekly Report [Dataset]. NADP Program Office. Retrieved from https://nadp.slh.wisc.edu/networks/national-trends-network/

Ng, N. L., Brown, S. S., Archibald, A. T., Atlas, E., Cohen, R. C., Crowley, J. N., et al. (2017). Nitrate radicals and biogenic volatile organic compounds: Oxidation, mechanisms, and organic aerosol. *Atmospheric Chemistry and Physics*, *17*(3), 2103–2162. https://doi.org/10.5194/acp-17-2103-2017

Nopmongcol, U., Beardsley, R., Kumar, N., Knipping, E., & Yarwood, G. (2019). Changes in United States deposition of nitrogen and sulfur compounds over five decades from 1970 to 2020. *Atmospheric Environment*, *209*, 144–151. https://doi.org/10.1016/j.atmosenv.2019.04.018

Park, R. J., Jacob, D. J., Field, B. D., Yantosca, R. M., & Chin, M. (2004). Natural and transboundary pollution influences on sulfate-nitrate-ammonium aerosols in the United States: Implications for policy. *Journal of Geophysical Research: Atmospheres*, *109*(D15). https://doi.org/10.1029/2003JD004473

Paulot, F., Jacob, D. J., Pinder, R. W., Bash, J. O., Travis, K., & Henze, D. K. (2014). Ammonia emissions in the United States, European Union, and China derived by high-resolution inversion of ammonium wet deposition data: Interpretation with a new agricultural emissions inventory (MASAGE_NH3). *Journal of Geophysical Research: Atmospheres*, *119*(7), 4343–4364. https://doi.org/10.1002/2013JD021130

Philip, S., Martin, R. V., & Keller, C. A. (2016). Sensitivity of chemistry-transport model simulations to the duration of chemical and transport operators: A case study with GEOS-Chem v10-01. *Geoscientific Model Development*, *9*(5), 1683–1695. https://doi.org/10.5194/gmd-9-1683-2016

Pye, H. O. T., Liao, H., Wu, S., Mickley, L. J., Jacob, D. J., Henze, D. K., & Seinfeld, J. H. (2009). Effect of changes in climate and emissions on future sulfate-nitrate-ammonium aerosol levels in the United States. *Journal of Geophysical Research: Atmospheres*, *114*(D1). https://doi.org/10.1029/2008JD010701

Ridley, D. A., Heald, C. L., & Ford, B. (2012). North African dust export and deposition: A satellite and model perspective. *Journal of Geophysical Research: Atmospheres*, *117*(D2). https://doi.org/10.1029/2011JD016794

Schindler, D. W. (1974). Eutrophication and recovery in experimental lakes: Implications for lake management. *Science*, *184*(4139), 897–899. https://doi.org/10.1126/science.184.4139.897

Schwede, D. B., & Lear, G. G. (2014). A novel hybrid approach for estimating total deposition in the United States. *Atmospheric Environment*, *92*, 207–220. https://doi.org/10.1016/j.atmosenv.2014.04.008

Seinfeld, J. H., & Pandis, S. N. (1998). *Atmospheric chemistry and physics: From air pollution to climate change*. John Wiley & Sons.

Sickles, J. E., II, & Shadwick, D. S. (2015). Air quality and atmospheric deposition in the eastern US: 20 years of change. *Atmospheric Chemistry and Physics*, *15*(1), 173–197. https://doi.org/10.5194/acp-15-173-2015

Silvern, R. F., Jacob, D. J., Mickley, L. J., Sulprizio, M. P., Travis, K. R., Marais, E. A., et al. (2019). Using satellite observations of tropospheric NO_2 columns to infer long-term trends in US NO_x emissions: The importance of accounting for the free tropospheric NO_2 background. *Atmospheric Chemistry and Physics*, *19*(13), 8863–8878. https://doi.org/10.5194/acp-19-8863-2019

Tan, J., Fu, J. S., & Seinfeld, J. H. (2020). Ammonia emission abatement does not fully control reduced forms of nitrogen deposition. *Proceedings of the National Academy of Sciences*, *117*(18), 9771–9775. https://doi.org/10.1073/pnas.1920068117

Travis, K. R., Crawford, J. H., Chen, G., Jordan, C. E., Nault, B. A., Kim, H., et al. (2022). Limitations in representation of physical processes prevent successful simulation of $PM_{2.5}$ during KORUS-AQ. *Atmospheric Chemistry and Physics*, *22*(12), 7933–7958. https://doi.org/10.5194/acp-22-7933-2022

Travis, K. R., Jacob, D. J., Fisher, J. A., Kim, P. S., Marais, E. A., Zhu, L., et al. (2016). Why do models overestimate surface ozone in the Southeast United States? *Atmospheric Chemistry and Physics*, *16*(21), 13561–13577. https://doi.org/10.5194/acp-16-13561-2016

US EPA. (1998). *National Air Pollutant Emission Trends, Procedures Document 1900-1996 (No. EPA-454/R-98-008)*. Research Triangle Park, NC: United States Environmental Protection Agency. Retrieved from https://www.epa.gov/sites/default/files/2015-07/documents/trends_procedures_old.pdf

US EPA. (2001a). *National Air Quality and Emissions Trends Report, 1999 (No. EPA 454/R-01-004)*. Research Triangle Park, NC: United States Environmental Protection Agency. Retrieved from https://www.epa.gov/sites/default/files/2017-11/documents/trends_report_1999.pdf

US EPA. (2001b). *Procedures Document For National Emission Inventory Criteria Air Pollutants 1985-1999 (No. EPA-454/R-01-006)*. Research Triangle Park, NC: United States Environmental Protection Agency. Retrieved from https://www.epa.gov/sites/default/files/2015-07/documents/aerr_final_rule.pdf

US EPA. (2015). *2011 National Emissions Inventory, version 2 Technical Support Document*. United States Environmental Protection Agency. Retrieved from https://www.epa.gov/air-emissions-inventories/2011-national-emissions-inventory-nei-technical-support-document

US EPA. (2021). *Our Nation's Air: Status and Trends Through 2020*. United States Environmental Protection Agency. Retrieved from https://gispub.epa.gov/air/trendsreport/2021/documentation/AirTrends_Flyer.pdf

US EPA. (2022). *National Tier 1 CAPs Trends (Air Pollutant Emissions Trends Data)*. United States Environmental Protection Agency. Retrieved from https://www.epa.gov/air-emissions-inventories/air-pollutant-emissions-trends-data

Walker, J. M., Philip, S., Martin, R. V., & Seinfeld, J. H. (2012). Simulation of nitrate, sulfate, and ammonium aerosols over the United States. *Atmospheric Chemistry and Physics*, *12*(22), 11213–11227. https://doi.org/10.5194/acp-12-11213-2012

Wang, X., Jacob, D. J., Downs, W., Zhai, S., Zhu, L., Shah, V., et al. (2021). Global tropospheric halogen (Cl, Br, I) chemistry and its impact on oxidants. *Atmospheric Chemistry and Physics*, *21*(18), 13973–13996. https://doi.org/10.5194/acp-21-13973-2021

Wang, Y., Jacob, D. J., & Logan, J. A. (1998). Global simulation of tropospheric O_3-NO_x -hydrocarbon chemistry: 1. Model formulation. *Journal of Geophysical Research: Atmospheres*, *103*(D9), 10713–10725. https://doi.org/10.1029/98JD00158

Wang, Y. X., McElroy, M. B., Jacob, D. J., & Yantosca, R. M. (2004). A nested grid formulation for chemical transport over Asia: Applications to CO. *Journal of Geophysical Research: Atmospheres*, *109*(D22). https://doi.org/10.1029/2004JD005237

Weng, H., Lin, J., Martin, R., Millet, D. B., Jaeglé, L., Ridley, D., et al. (2020). Global high-resolution emissions of soil NO_x, sea salt aerosols, and biogenic volatile organic compounds. *Scientific Data*, *7*(1), 148. https://doi.org/10.1038/s41597-020-0488-5

Wesely, M. L. (1989). Parameterization of surface resistances to gaseous dry deposition in regional-scale numerical models. *Atmospheric Environment*, *23*(6), 1293–1304. https://doi.org/10.1016/0004-6981(89)90153-4

Zhang, L., Gong, S., Padro, J., & Barrie, L. (2001). A size-segregated particle dry deposition scheme for an atmospheric aerosol module. *Atmospheric Environment*, *35*(3), 549–560. https://doi.org/10.1016/S1352-2310(00)00326-5

Zhang, L., Jacob, D. J., Knipping, E. M., Kumar, N., Munger, J. W., Carouge, C. C., et al. (2012). Nitrogen deposition to the United States: Distribution, sources, and processes. *Atmospheric Chemistry and Physics*, *12*(10), 4539–4554. https://doi.org/10.5194/acp-12-4539-2012

Zhang, Y., Foley, K. M., Schwede, D. B., Bash, J. O., Pinto, J. P., & Dennis, R. L. (2019). A measurement-model fusion approach for improved wet deposition maps and trends. *Journal of Geophysical Research: Atmospheres*, *124*(7), 4237–4251. https://doi.org/10.1029/2018JD029051